Articles in PresS. Am J Physiol Heart Circ Physiol (November 25, 2015). doi:10.1152/ajpheart.00754.2015

Early Detection of Acute Transmural Myocardial Ischemia by the Phasic Systolic- Diastolic Changes of Local Tissue Electrical Impedance

Esther Jorge[1]*, Gerard Amorós-Figueras[1]*, Tomás García-Sánchez[2], Ramón Bragós[2], Javier Rosell-Ferrer[2], Juan Cinca[1]

[1]Department of Cardiology, Hospital de la Santa Creu i Sant Pau, IIB-Sant Pau, Universitat Autonoma de Barcelona, Barcelona, Spain.

[2] Electronic and Biomedical Instrumentation Group, Department of Electronics Engineering,Universitat Politecnica de Catalunya (UPC), Barcelona, Spain.

*both authors contributed equally to this work

Running title: Ischemia Induced Systolic-Diastolic Resistivity Changes

Address for correspondence:

Esther Jorge, Department of Cardiology, Hospital de la Santa Creu i Sant Pau, Sant Antoni MªClaret, 167, 08025, Barcelona, Spain. Phone: (+34) 935537058 Fax number: (+34) 935565603 E-mail address: ejorge@santpau.cat

ABSTRACT

Myocardial electrical impedance is influenced by the mechanical activity of the heart. Therefore, the ischemia induced mechanical dysfunction may cause specific changes in the systolic-diastolic pattern of myocardial impedance but this is not known. This study aimed to analyze the phasic changes of myocardial resistivity in normal and ischemic conditions. Myocardial resistivity was measured continuously during the cardiac cycle using 26 different simultaneous excitation frequencies (1 kHz-1 MHz) in 7 anesthetized open chest pigs. Animals were submitted to 30 minutes regional ischemia by acute left anterior descending coronary artery occlusion. The electrocardiogram, left ventricular (LV) pressure, LV dP/dt and aortic blood flow were recorded simultaneously. Baseline myocardial resistivity depicted a phasic pattern during the cardiac cycle with higher values at the pre-ejection period (4.19±1.09% increase above the mean,$p<0.001$) and lower values during relaxation phase (5.01±0.85% below the mean,$p<0.001$). Acute coronary occlusion induced two effects on the phasic resistivity curve: 1) a prompt (5 min ischemia) holosystolic resistivity rise leading to a bell-shaped waveform and to a reduction of the area under the LV pressure-impedance curve (1427±335 Ω·cm·mmHg vs 757±266 Ω·cm·mmHg,$p<0.01$,41 kHz) and 2) a subsequent (5-10 min ischemia) progressive mean resistivity rise (325±23 Ω·cm vs 438±37 Ω·cm at 30 min,$p<0.01$,1 kHz). The structural and mechanical myocardial dysfunction induced by acute coronary occlusion can be recognized by specific changes in the systolic-diastolic myocardial resistivity curve. Therefore these changes may become a new indicator (surrogate) of evolving acute myocardial ischemia.

48 **NEW & NOTEWORTHY**

49 This study affords a new method to promptly recognize the presence of acute
50 myocardial ischemia based on the measurement of the local changes in myocardial
51 resistivity elicited during heart contraction and relaxation.

52

53 **KEYWORDS**

54 animal model; bioelectrical impedance; hemodynamics; myocardial ischemia.

55

56

57

INTRODUCTION

Myocardial electrical resistivity is a passive biophysical property of the heart that is influenced by geometrical cell characteristics and by the structural integrity of the myocardium (16). Classical measurements of myocardium electrical resistivity have usually been performed at a single current frequency, in the 1 kHz - 15 kHz range (6) or using the frequency-sweep Electrical Impedance Spectroscopy (EIS) technique, in the 0.1 kHz - 10 MHz range (8) or in the 1 kHz - 1 MHz range (12). With these techniques, stationary characterization of myocardial resistivity in normal and ischemic myocardium was possible (20), but due the time required for the whole impedance spectrum acquisition, only few measurements could be drawn during the cardiac cycle. Therefore, the phasic changes in myocardial resistivity that are close linked to the mechanical activity of the beating heart were not well defined.

Recently, with the use of the fast broadband EIS, it is feasible to obtain up to 1,000 spectrums/s and therefore a more refined information about the time behavior of myocardial impedance during the mechanical cardiac activity. It is predictable that in the presence of acute myocardial ischemia the resultant structural and mechanical derangements will exert specific changes in the phasic systolic-diastolic resistivity curve, but this is not known.

This study aimed to characterize the phasic (systolic-diastolic) changes of myocardial resistivity in normal and ischemic conditions in the in situ pig heart by using fast broadband EIS.

MATERIALS AND METHODS

Study population

Seven female domestic swine (Landrace-Large White cross) weighing 40 kg were premedicated with a combination of midazolam (0.6 mg/kg) and ketamine (12 mg/kg), both injected intramuscularly. Anesthesia was induced with intravenous propofol (2-4 mg/kg). After endotracheal intubation, general anesthesia was maintained with sevofluorane inhalation (2.5-3.5 % with oxygen) and the animals were mechanically ventilated. Ventilatory parameters were adjusted to maintain blood gases within physiological ranges. Remifentanyl (0.2 mcg/kg/min) was administered during the procedure for analgesia.

The study protocol was approved by the Institutional Animal Care and Use Committee (IACUC) of our institution, and conformed to the regulation for the treatment of animals established by the *Guide for the Care and Use of Laboratory Animals*: Eighth Edition (National Research Council. Washington, DC: the National Academies Press, 2010).

Experimental preparation

A femoral arterial access was established by using the Seldinger technique and a 6F introducer sheath (Cordis Corp., Florida, USA) was introduced percutaneously into the femoral artery. Under fluoroscopic guidance, a 5F Millar micromanometer catheter (Millar Instruments, Inc., Houston, TX, USA) was advanced to the left ventricle (LV) to continuously monitor the LV pressure. The peripheral electrocardiogram (ECG) was recorded (Nihon Kohden Corporation, Japan). The thorax was opened through a midline sternotomy, and the heart was suspended in a pericardial cradle. An ultrasonic flow probe (Transonic Systems Inc., Ithaca, NY, US) was carefully deployed around the aortic root to monitor the aortic

blood flow (ABF). The left anterior descending (LAD) coronary artery was dissected after the first diagonal and was looped with a Prolene 3/0 snare (Ethicon Inc., New Jersey, US).

Electrocardiographic and hemodynamic parameters

In all cases, we recorded the following signals: a) the conventional ECG lead II, b) the LV pressure with an intracavitary Millar micromanometer catheter, and c) ABF. An amplifier system Nihon Kohden Corporation was used to record the LV pressure and ECG and a Transonic Systems Inc. to construct the ABF curve. All signals were digitized at 1 kHz (PowerLab with LabChart, ADInstruments Pty.Ltd, Australia) and stored for subsequent offline analysis. The first derivative of LV pressure was also calculated.

Myocardial electrical impedance

Theoretical background. The whole myocardial electrical impedance is an overall estimation of the intra- and extracellular resistances and the cell membrane capacitance (7). Impedance (Z) is defined as the voltage (V) divided by the sinusoidal current (I) of a given frequency (f) applied through a region ($Z(f)=V/I$). Since biological tissues are not purely resistive, there will be a time delay (Δt) between the voltage and current waves which is measured as a phase angle shift ($\Theta=360\cdot\Delta t\cdot f$). Therefore, myocardial impedance has two components: tissue resistivity (ρ) and phase angle (Θ). Tissue resistivity was calculated from the relation $R=k\rho$, where R is the in phase component of V with respect to I, and k is the cell constant of the electrode determined by measuring the electrical resistance of a 0.9% NaCl solution at 25ºC, which affords a resistivity of 70 Ω·cm.

Tissue Impedance Spectroscopy. Tissue impedance was measured with a four-electrode probe to minimize the electrode–tissue interface impedance (17). The

probe consisted of a linear array of four platinum-iridium needle electrodes (5 mm long, 0.4 mm diameter, with a constant interelectrode distance of 1.27 mm). The outer pair of electrodes were used to apply the test currents to the myocardium, while the inner two electrodes were employed to measure the resulting potential difference. The electrode probe was inserted into the LV myocardial wall, perpendicular to the trajectory of the LAD coronary artery (Figure 1). An analog front-end was used to interconnect the electrode array with the signal generation and acquisition system. The impedance measurements were performed using a current excitation consisting of a multisine signal (1 ms duration, 1 mA peak amplitude) of 26 frequencies logarithmically spaced in the range from 1 kHz to 1 MHz, obtaining 1000 spectra/s. Both current generation and acquisition were synchronized using a custom setup based on a PXI system from National Instruments. The acquired signals were low-pass filtered and then digitized at 5 MHz sampling rate. The physiological signals (LV pressure, ABF, ECG) were acquired synchronously with the impedance measurements, using an additional 8-channel digitizer card included in the PXI system. To compensate for the potential error effects elicited by the cables and the amplifier response, the electrical impedance setup was calibrated at the beginning of each study by measuring the impedance spectrum of a test saline solution of known resistivity.

We have analyzed the time course of the resistivity patterns during 3 phases of the cardiac cycle: pre-ejection (1), ejection (2) and relaxation (3). The pre-ejection phase was defined as the interval between the peak of the R wave of the ECG to the start of the steep increase of the ABF (aortic valve opening); the ejection phase was delimited between the last point of previous phase and the moment where ABF dropped rapidly towards zero L/min (aortic valve closure); and the relaxation phase

was defined as the rest of the cycle until the next R wave peak. We measured the maximum value of the resistivity during the pre-ejection phase, the mean value of the resistivity during the ejection phase and the minimum value of the resistivity during the relaxation phase at baseline and after coronary occlusion. These measures were performed in 3 consecutive cardiac cycles and data were averaged for statistical analysis. The resistivity values were normalized to their relative change from the total resistivity mean: ($\Delta Z=100*(Z_{ph} -Z_{mean})/Z_{mean}$). Further analyses of resistivity changes in relation to the LV pressure (pressure-impedance curves) were also performed.

Study protocol

The study began after stabilization of the anesthesia level and hemodynamic parameters. Then, the hemodynamic and electrical signals were recorded at baseline and sequentially during 30 min of acute transmural myocardial ischemia in the territory of the implanted impedance electrode by occluding the LAD coronary artery. At the end of the study the animals were euthanized and the heart was removed to verify the appropriate location of the impedance electrode in the ischemic region.

Statistical analysis

Data were expressed as mean ± standard error of the mean (SEM). Differences in the study variables were assessed using repeated measures t-test, and analysis of variance (ANOVA) with Bonferroni correction for post-hoc comparisons, as appropriate. A p value of <0.05 was considered statistically significant. Statistical analyses were performed using the software SPSS v.22.0 (IBM SPSS Inc., Chicago, IL, USA).

RESULTS

ECG and Hemodynamic parameters

As shown in Figure 1, LAD occlusion induced a visible area of cyanosis in the subtended myocardial region, which was associated with reciprocal ST segment depression in lead II, and a decrease of the LV systolic pressure, negative LV dP/dt, and aortic blood flow (Table 1 and Figure 2). The positive LV dP/dt also followed a decreasing tendency , but this was not statistically significant.

Phasic changes in myocardial impedance

As illustrated in Figure 3A, electrical resistivity of the normal myocardium depicted phasic changes during the cardiac cycle: a maximal value was attained during the pre-ejection period and a minimal value during the relaxation phase. The lower panel in Figure 3A shows the phasic changes in resistivity at various frequencies expressed as % variation from the mean value in the 7 studied pigs. This analysis indicated that during the pre-ejection period the resistivity at 41 kHz increased by 4.19±1.09% ($p<0.001$) over the mean, whereas a decrease of about 5.01±0.85 % ($p<0.001$) occurred during the relaxation phase. The phasic pattern of resistivity changes was valid for all test current frequencies analyzed.

Acute LAD occlusion induced remarkable changes in both the shape of the phasic pattern and magnitude of local tissue resistivity (Figures 3B and 3C). As shown in Figure 3B, soon after coronary occlusion the resistivity curve recorded in the ischemic region evolved to a bell-shaped contour as a result of a sustained resistivity rise that persisted throughout the whole ejection phase. The lower panel of the figure 3 illustrates the phasic changes at various frequencies in the whole experimental series. Thus, at 5 min of LAD occlusion the % change over the mean resistivity at 41 kHz was 3.14±0.97% at pre-ejection ($p<0.001$); 2.24±0.64% during

ejection ($p<0.001$); and -6.42±0.89% during the relaxation phase ($p<0.001$). Thereafter, the changes in the resistivity pattern were accompanied by a progressive increase in the magnitude of the whole tissue resistivity as illustrated in Figure 3C. At 30 min of LAD occlusion the mean resistivity increased significantly at 1 kHz and 41 kHz (from 325±23 Ω·cm to 438±37 Ω·cm, $p<0.001$, at 1 kHz and from 276±21 Ω·cm to 339±27 Ω·cm, $p<0.01$, at 41 kHz).

Myocardial impedance spectroscopy

Figure 4 illustrates the dependence of myocardial resistivity and its phase angle on the frequency of the injected alternating current. In normal conditions (Figure 4A), the magnitude of myocardial resistivity (solid line represents the mean values and dash lines the maximum and minimum values of the whole phasic changes) decreased as the frequency increased (from 325±23 Ω·cm at 1 kHz to 213±17 Ω·cm at 1 MHz, $p<0.001$). Under ischemic conditions, myocardial resistivity followed a similar trend of changes (from 438±37 Ω·cm at 1 kHz to 231±18 Ω·cm at 1 MHz, $p<0.001$) although with a greater mean value (mean resistivity rise of about 23% at 41 kHz, $p<0.01$).

The lower panels in Figure 4 illustrate the frequency dependence of the phase angle of myocardial impedance. In the nonischemic myocardium the phase angle followed a progressive decline to more negative values as the frequency of the injected current was increased from 1 kHz to 300 kHz. At frequencies higher than 300 kHz, the phase angle depicted less negative values. In the presence of acute myocardial ischemia the phase angle evolved to more negative values than baseline at all current frequencies. Moreover, the figure shows a deepest deviation at 300 kHz and a new relaxation at 5-10 kHz. The current frequencies that better differentiate the resistivity of the healthy and acute ischemic myocardium were those comprised

between 1 kHz to 41 kHz. By contrast, the phase angle changes are better differentiated at frequencies ranging from 41 kHz to 1 MHz.

LV pressure-impedance curves

The temporal relationship between the whole cardiac mechanical activity and the concurrent changes in regional myocardial impedance can be better analyzed by constructing the LV pressure-impedance loop (Figure 5B). This shows that during the pre-ejection phase (segment #1 in Figure 5) both the LV pressure and myocardial resistivity increased progressively. However, during the ejection phase (segment #2) resistivity dropped rapidly while the LV pressure remained rather stationary. At the beginning of the relaxation phase (segment #3) both the LV pressure and resistivity decreased progressively but at the end of this period, when the LV pressure dropped to nearly 0 mmHg, the resistivity increased rapidly to the pre-ejection value.

The LV pressure-impedance loop suffered marked changes during acute LAD occlusion. As illustrated in Figure 6, the area under the LV pressure-impedance curve (AUC) decreased dramatically 5 min after LAD occlusion (from 1427±335 Ω·cm·mmHg to 733±157 Ω·cm·mmHg at 41 kHz, $p<0.01$). This figure reveals that the AUC reduction is likely caused by the lack of changes in resistivity during the plateau rise at the ejection phase. Likewise, the progressive increase in the magnitude of resistivity that was detected in the ensuing stages of ischemia shifted the LV pressure-resistivity loop upwards to higher resistivity values. Figure 6 illustrates the shift of the depressed loop at 30 min of LAD occlusion (AUC: 1427±335 Ω·cm·mmHg vs. 757±266 Ω·cm·mmHg at 41 KHz $p<0.01$). The shape of the LV pressure-impedance loops was comparable among the different current frequencies analyzed in this study.

DISCUSSION

Main findings

This study shows that acute transmural myocardial ischemia exerts two well defined effects on local tissue electrical impedance. One effect was already known and consisted of a myocardial resistivity rise that became significant after 5-10 min of ischemia (11, 20). The second effect, which has not been previously reported, was characterized by a fast change in the contour of the local systolic-diastolic resistivity curve. Specifically, within the first 5 min of ischemia the resistivity curve evolved from a biphasic pattern -with higher values at pre-ejection phase and lower values during relaxation- to a bell-shaped contour caused by a sustained resistivity rise during systole. This local holosystolic sustained resistivity rise shared a close time-relationship with the local mechanical systolic bulging that develops during the first minutes of interruption of the LAD coronary flow in the ischemic region, also in the pig heart model I (3). Therefore, this study suggests a close relationship between the morphology of the phasic myocardial resistivity curve obtained by continuous measurement of the tissue resistivity during the cardiac cycle and the local mechanical cardiac activity.

Mechanism of the phasic changes in myocardial impedance

The phasic changes in myocardial resistivity are likely related to the cyclic variations of myocardial cell geometry that occur during cardiac contraction and relaxation. This assumption is based on the fact that myocardial impedance is modulated by changes in cell dimension and structural integrity (16) and, on the other hand, on the observation that cardiac contraction and relaxation induce cyclic changes in myocardial thickness (19) and cell length (2).

Recording of the phasic resistivity curve was not feasible until recently. The inability to detect specific impedance differences between systole and diastole was alluded by previous investigators (6, 10) and was mainly due to the low sampling rate imposed by the impedance measuring system. Recently, we (13, 14) reported a novel methodological procedure allowing to detect the evolving temporal changes of bioimpedance during the cardiac cycle by using fast broadband electrical impedance spectroscopy (EIS). Thus, we were able to acquire up to 1,000 spectra per second in healthy porcine myocardium although in that study we could not fully characterize the phasic resistivity curve due to the lack of synchronized physiological parameters. Using the frequency-sweep EIS technique in healthy tissue other authors (17) reported impedance changes during the cardiac cycle in relation to the myocardial fiber orientation: higher longitudinal resistivity values during the ejection phase and higher transverse resistivity values during late diastole. In our study myocardial resistivity was higher in the pre-ejection phase and lower during diastole. These two studies used distinct measurement techniques: a contact epicardial probe in the first study and a four needle electrode inserted 5 mm deep into the myocardium in ours. The intramural electrode encompasses the different myocardial layers of the ventricular wall and would be expected to average the effects of layer fiber orientation. In addition, in the study by Steendijk et al. the impedance spectrum (8 current frequencies) was measured stepwise during 30 seconds and as a consequence of the large measuring time required, the temporal variation of the bioimpedance spectrum during the cardiac cycle might be underestimated.

The myocardial structure consists of two electrically conducting compartments (the intra and extracellular spaces) separated by insulating membranes. The conductance of the electric current flowing through this structure is highly dependent

on the current frequency (8, 12, 20). The present study shows that the average specific myocardial impedance is frequency dependent in the 1 kHz-1 MHz range, but the phasic changes of resistance during the cardiac cycle are not. These observations suggest that the impedance is mainly modulated by the structural and/or morphological changes, whereas the impedance waveform is highly synchronized with changes in wall thickness as reported by Sasaki et al. (15)

Myocardial ischemia causes intracellular edema and this results in cellular enlargement and extracellular space volume reduction (18, 21). Under these conditions the average impedance increases at all studied frequencies as reported previously by us and others (4, 6, 12). In addition, our results showed that the frequencies that better differentiate normal from ischemic tissue are 1 and 41 kHz for the resistance and 300 kHz for the phase angle.

LV pressure-impedance curves

We analyzed the temporal relationship between the cyclic changes in myocardial resistivity and the concurrent level of LV pressure by constructing the LV pressure-impedance loop. Establishing a parallelism with the well-known pressure-volume curve that reflects the whole work performed by the corresponding ventricle (1) then, the LV pressure-impedance loop would indicate the LV resistance strength referred to a particular explored area. As a novel contribution our study shows that early after coronary occlusion the area under the LV pressure-impedance began to decrease dramatically and therefore this parameter will further contribute to recognize acute myocardial ischemia. The virtual abolition of the area under the LV pressure-impedance curve during the first 5 minutes of ischemia was due to the lack of resistivity decrease during the ejection period. Lyseggen et al. (9) studied the relationship between LV pressure and local segment length (SL), and observed that

328 regions with depressed motility, characterized by regional work close to 0, showed
329 reduced LV pressure-SL area.

330 Thus, our findings suggest that the LV pressure-impedance loop would allow
331 differentiating the segments that generate active force (healthy tissue) from those
332 ischemic dyskinetic segments that are entirely passive. In fact, active myocardial
333 regions with cell contraction contribute to the pressure changes, whereas passive
334 regions with ischemia-induced local dyskinesis, are not contributing to pressure
335 generation and instead, they suffer tissue deformation as a consequence of the
336 whole intraventricular pressure changes generated by the cardiac beat.

337 **Considerations on the model**

338 The systolic-diastolic impedance patterns described in this study were
339 recorded with intramural needle electrodes in the open chest swine model. Although
340 the direct intramyocardial measurements are the most appropriate for a refined
341 detection of the local tissue resistivity changes, this is an invasive approach which on
342 the other hand required a thoracotomy. An intracavitary approach based on an
343 endocardial contact electrocatheter probe is theoretically feasible and would
344 overcome these limitations. Indeed, we have previously reported in the same
345 experimental model, that the myocardial resistivity changes induced by coronary
346 occlusion can be successfully detected with an electrocatheter based approach in
347 the closed chest (5).

348

Conclusions

Acute transmural myocardial ischemia can be promptly recognized by specific changes in the systolic-diastolic pattern of local electrical myocardial resistivity.

GRANTS

This work was supported by grants from Spanish Ministerio de Economía y Competitividad, Instituto de Salud Carlos III and Fondo Europeo de Desarollo Regional (FEDER): FIS-PI13/00765 and RIC-RD12/0042/0002, Red de Investigación Cardiovascular (Redes Temáticas de Investigación Cooperativa en Salud - RETICS).

DISCLOSURES

No conflicts of interest, financial or otherwise, are declared by the author(s).

AUTHOR CONTRIBUTIONS

J.C., R.B. and J.R.-F. conception and design of research; E.J., G.A.-F., T.G.-S., R.B., J.R.-F. and J.C. performed experiments; E.J. and G.A.-F. analyzed data; E.J., G.A.-F. and J.C. interpreted results of experiments; E.J. and G.A.-F. prepared figures; E.J., G.A.-F. and J.C. drafted manuscript; E.J., G.A.-F., T.G.-S., R.B., J.R.-F. and J.C. edited and revised manuscript.; E.J., G.A.-F., T.G.-S., R.B., J.R.-F. and J.C. approved final version of manuscript.

REFERENCES

1. **Baan J, van der Velde ET, de Bruin HG, Smeenk GJ, Koops J, van Dijk AD, Temmerman D, Senden J, Buis B**. Continuous measurement of left ventricular volume in animals and humans by conductance catheter. *Circulation* 70: 812–823, 1984.

2. **Bramlage P, Joss G, Staudt A, Jarrin A, Podlowski S, Baumann G, Stangl K, Felix SB, Stangl V**. Computer-aided measurement of cell shortening and calcium transients in adult cardiac myocytes. *Biotechnol Prog* 17: 929–934, 2001.

3. **Cinca J, Carreño A, Mont L, Blanch P, Soler-Soler J**. Neurally mediated negative inotropic effect impairs myocardial function during cholinergic coronary vasoconstriction in pigs. *Circulation* 94: 1101–1108, 1996.

4. **Cinca J, Warren M, Carreño A, Tresànchez M, Armadans L, Gómez P, Soler-Soler J**. Changes in myocardial electrical impedance induced by coronary artery occlusion in pigs with and without preconditioning: correlation with local ST-segment potential and ventricular arrhythmias. *Circulation* 96: 3079–3086, 1997.

5. **Cinca J, Warren M, Rodríguez-Sinovas A, Tresànchez M, Carreño A, Bragós R, Casas O, Domingo A, Soler-Soler J**. Passive transmission of ischemic ST segment changes in low electrical resistance myocardial infarct scar in the pig. *Cardiovasc Res* 40: 103–112, 1998.

6. **Fallert MA, Mirotznik MS, Downing SW, Savage EB, Foster KR, Josephson ME, Bogen DK**. Myocardial electrical impedance mapping of ischemic sheep hearts and healing aneurysms. *Circulation* 87: 199–207, 1993.

7. **Gebhard MM, Gersing E, Brockhoff CJ, Schnabel PA, Bretschneider HJ**. Impedance spectroscopy: a method for surveillance of ischemia tolerance of the heart. *Thorac Cardiovasc Surg* 35: 26–32, 1987.

8. **Gersing E**. Impedance spectroscopy on living tissue for determination of the state of organs. *Bioelectrochemistry Bioenerg* 45: 145–149, 1998.

9. **Lyseggen E, Skulstad H, Helle-Valle T, Vartdal T, Urheim S, Rabben SI, Opdahl A, Ihlen H, Smiseth OA**. Myocardial strain analysis in acute coronary occlusion: A tool to assess myocardial viability and reperfusion. *Circulation* 112: 3901–3910, 2005.

10. **Van Oosterom A, de Boer RW, van Dam RT**. Intramural resistivity of cardiac tissue. *Med Biol Eng Comput* 17: 337–43, 1979.

11. **Padilla F, Garcia-Dorado D, Rodríguez-Sinovas A, Ruiz-Meana M, Inserte J, Soler-Soler J**. Protection afforded by ischemic preconditioning is not mediated by effects on cell-to-cell electrical coupling during myocardial

406 ischemia-reperfusion. *Am J Physiol Heart Circ Physiol* 285: H1909–H1916,
407 2003.

408 12. **Salazar Y, Bragos R, Casas O, Cinca J, Rosell J**. Transmural versus
409 nontransmural in situ electrical impedance spectrum for healthy, ischemic, and
410 healed myocardium. *IEEE Trans Biomed Eng* 51: 1421–1427, 2004.

411 13. **Sanchez B, Louarroudi E, Jorge E, Cinca J, Bragos R, Pintelon R**. A new
412 measuring and identification approach for time-varying bioimpedance using
413 multisine electrical impedance spectroscopy. *Physiol Meas* 34: 339–357, 2013.

414 14. **Sanchez B, Schoukens J, Bragos R, Vandersteen G**. Novel estimation of
415 the electrical bioimpedance using the local polynomial method. Application to
416 in vivo real-time myocardium tissue impedance characterization during the
417 cardiac cycle. *IEEE Trans Biomed Eng* 58: 3376–3385, 2011.

418 15. **Sasaki E, Conger JL, Kadipasaoglu KA, Pehlivanoglu S, Frazier OH**.
419 Simultaneous evaluation of cardiac wall motion and myocardial ischemic injury
420 by measurement of electrical impedance. *ASAIO J* 40: M826–9.

421 16. **Sperelakis N, Hoshiko T**. Electrical impedance of cardiac muscle. *Circ Res* 9:
422 1280–1283, 1961.

423 17. **Steendijk P, Van der Velde ET, Baan J**. Dependence of anisotropic
424 myocardial electrical resistivity on cardiac phase and excitation frequency.
425 *Basic Res Cardiol* 89: 411–426, 1994.

426 18. **Tranum-Jensen J, Janse MJ, Fiolet WT, Krieger WJ, D'Alnoncourt CN,**
427 **Durrer D**. Tissue osmolality, cell swelling, and reperfusion in acute regional
428 myocardial ischemia in the isolated porcine heart. *Circ Res* 49: 364–381, 1981.

429 19. **Troy BL, Pombo J, Rackley CE**. Measurement of left ventricular wall
430 thickness and mass by echocardiography. *Circulation* 45: 602–611, 1972.

431 20. **Warren M, Bragós R, Casas O, Rodríguez-Sinovas A, Rosell J, Anivarro I,**
432 **Cinca J**. Percutaneous electrocatheter technique for on-line detection of
433 healed transmural myocardial infarction. *Pacing Clin Electrophysiol* 23: 1283–
434 1287, 2000.

435 21. **Whalen DA, Hamilton DG, Ganote CE, Jennings RB**. Effect of a transient
436 period of ischemia on myocardial cells. I. Effects on cell volume regulation. *Am*
437 *J Pathol* 74: 381–397, 1974.

438

439 **FIGURE LEGENDS**

440 **Figure 1**. Schematic representation of the experimental model. A: shows a
441 photograph of the left ventricular anterior wall in an open chest pig heart preparation
442 submitted to occlusion (occl.) of the left anterior descending (LAD) coronary artery.
443 The dotted white line delineates the border between the cyanotic ischemic region
444 (IZ) and the non-ischemic myocardium (NZ). The impedance probe is inserted inside
445 the cyanotic region. B: shows a schematic representation of the system used to
446 record simultaneously the phasic changes of myocardial electrical impedance (Z),
447 left ventricular (LV) pressure, aortic blood flow (ABF) and surface ECG.

448

449 **Figure 2.** Simultaneous recording of myocardial resistivity at 1 kHz, left ventricular
450 (LV) pressure, LV dP/dt, aortic blood flow (ABF) and lead II of the ECG at baseline
451 (A), and after 5 minutes (B) and 30 minutes of LAD coronary occlusion (C).

452

453 **Figure 3.** Time course of the changes in myocardial resistivity during 30 minutes of
454 LAD occlusion at different current frequencies. Panel A (upper) shows the
455 simultaneous recording of baseline resistivity at 1 kHz, ECG and aortic blood flow
456 during the 3 different phases of the cardiac cycle: pre-ejection (1), ejection (2) and
457 relaxation (3), in one anesthetized pig. The lower panel shows the percentage
458 change from the mean resistivity value at different frequencies in the group of 7 pigs.
459 Five minutes after LAD occlusion (panel B) there was a plateau increase of resistivity
460 during the ejection period which was statistically significant in the group of 7 pigs
461 (lower panel). Panel C shows an increase in the myocardial resistivity (upward shift)
462 maintaining the bell-shaped contour seen at 5 minutes occlusion. ***=p<0,001 vs
463 mean.

Figure 4. Myocardial resistivity (upper) and phase angle (lower) at different frequencies (1 kHz-1 MHz) during baseline (A), and after 5 minutes (B) and 30 minutes of LAD occlusion (C) in one anesthetized pig. The solid line represents the mean values of the phasic resistivity changes and the dashed lines their maximum and minimum values. Signals in the inset boxes represent the phasic patterns of myocardial electrical resistivity at 41 kHz. Panel D shows the mean value of resistivity and phase angle for the whole group of 7 pigs at four specified excitation frequencies in baseline conditions and after 5 and 30 minutes of LAD occlusion. *** = p<0,001 ; ** = p<0,01, * = p<0.05.

Figure 5. Time relationship between the changes in myocardial impedance and left ventricular (LV) pressure (left panel) expressed graphically by the LV pressure-impedance curves (right panel) during the pre-ejection (1), ejection (2) and relaxation (3) phases of the cardiac cycle in one anesthetized pig.

Figure 6. Changes in the LV pressure-impedance curve during 30 minutes of LAD occlusion. Panel A shows a drop of the area under the LV pressure-impedance curve (AUC) soon after LAD occlusion (5 minutes) that was followed by an upright deviation towards higher myocardial resistivity values at 1 kHz after 30 minutes LAD occlusion in one anesthetized pig. Panel B shows the LV pressure-impedance curve AUC of the whole group of animals at different excitation frequencies at baseline and after 5 and 30 minutes of ischemia.
Loops are divided in three periods: pre-ejection (slim line), ejection (bold line) and relaxation (dashed line), **=p<0,01; *=p<0,05.

TABLES

Table 1.Hemodynamic parameters in seven anesthetized pigs submitted to 30 minutes of left anterior descending (LAD) coronary artery occlusion.

	Basal (n=7)	**30' LAD occl. (n=7)**	**p**
RR interval (ms)	842±63	804±74	ns
LVSP (mmHg)	83±4	76±4	<0,01
LVEDP (mmHg)	10,0±2	12±2	ns
dP/dt max ($mmHg \cdot s^{-1}$)	1410±94	1246±63	ns
dP/dt min ($mmHg \cdot s^{-1}$)	-1274±131	-1091±128	<0,01
ABF (L/min)	3,0±0,3	2,3±0,2	<0,05

Values are means ± SE; n = 7.
Abbreviations: LVSP: Left ventricular systolic pressure; LVEDP: Left ventricular end-diastolic pressure; dP/dt: First derivative of the left ventricular pressure; ABF:Aortic blood flow.

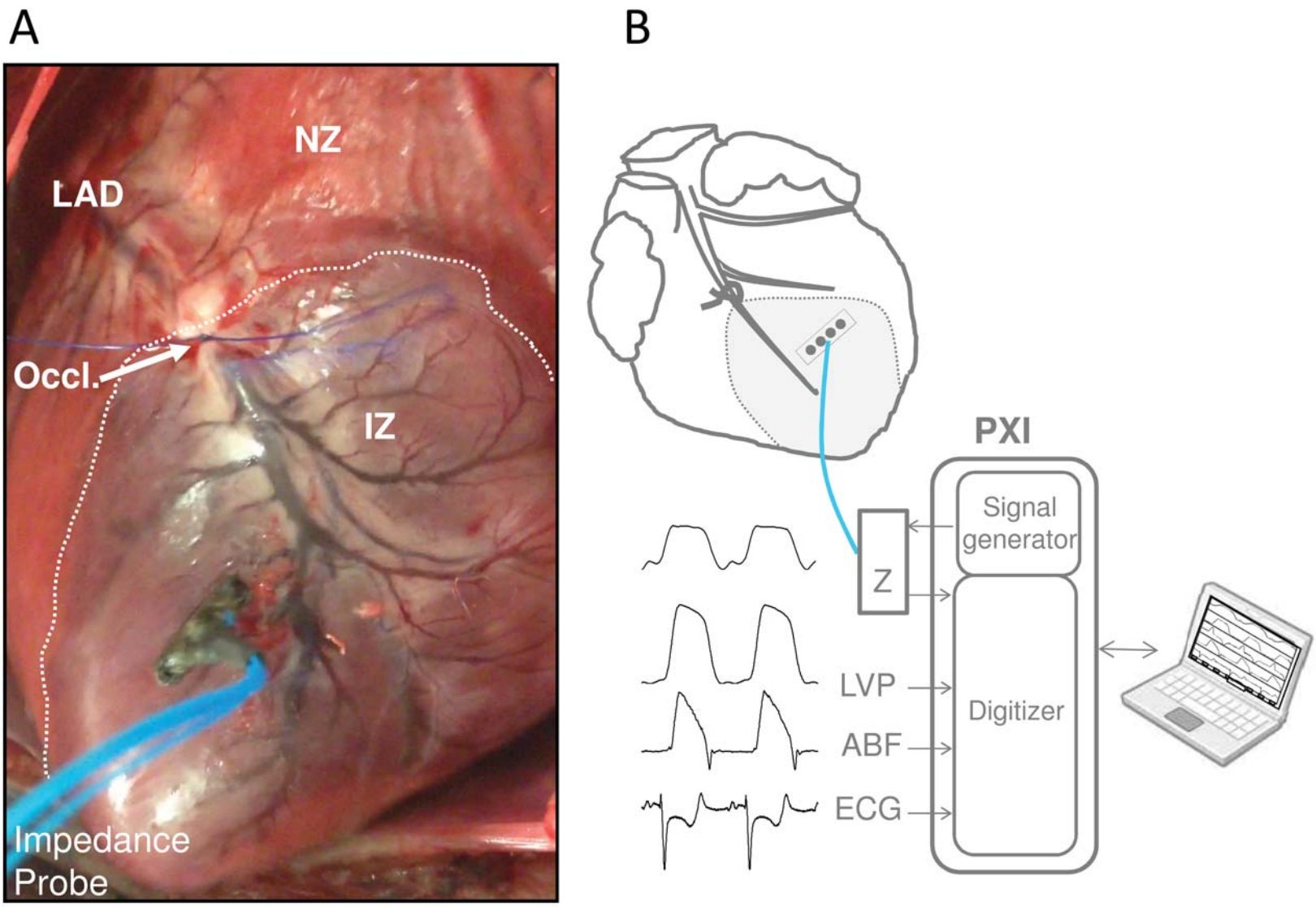
A
NZ
LAD
Occl.
IZ
Impedance
Probe
B
PXI
Signal
generator
Z
LVP
ABF
ECG
Digitizer

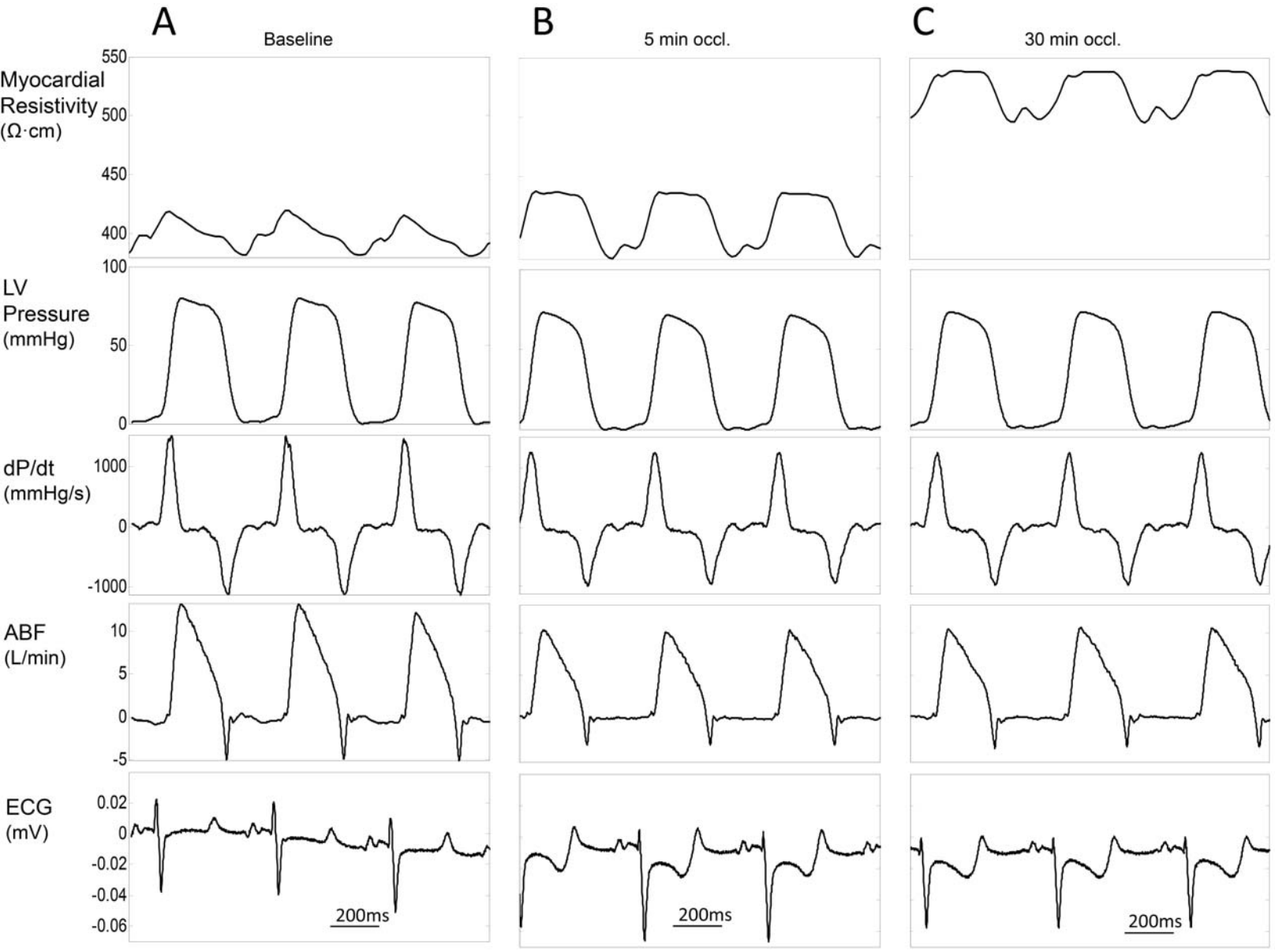
A
Baseline
B
5 min occl.
C
30 min occl.
Myocardial Resistivity (Ω·cm)
550
500
450
400
LV Pressure (mmHg)
100
50
0
dP/dt (mmHg/s)
1000
0
-1000
ABF (L/min)
10
5
0
-5
ECG (mV)
0.02
0
-0.02
-0.04
-0.06
200ms
200ms
200ms

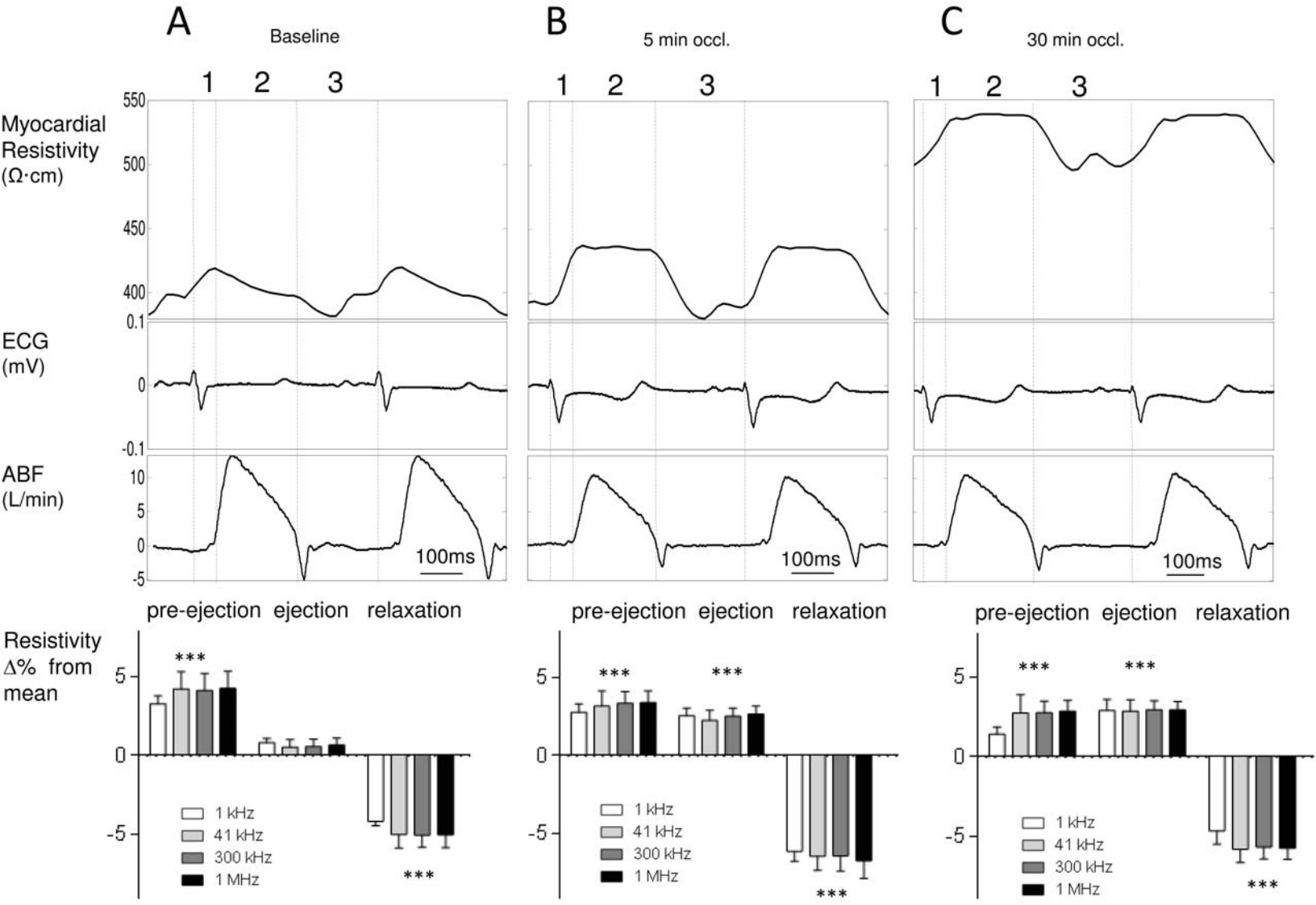
A
Baseline
B
5 min occl.
C
30 min occl.
1 2 3
Myocardial Resistivity (Ω·cm)
550
500
450
400
ECG (mV)
0.1
0
-0.1
ABF (L/min)
10
5
0
-5
100ms
pre-ejection ejection relaxation
Resistivity Δ% from mean
5
0
-5
***
1 kHz
41 kHz
300 kHz
1 MHz

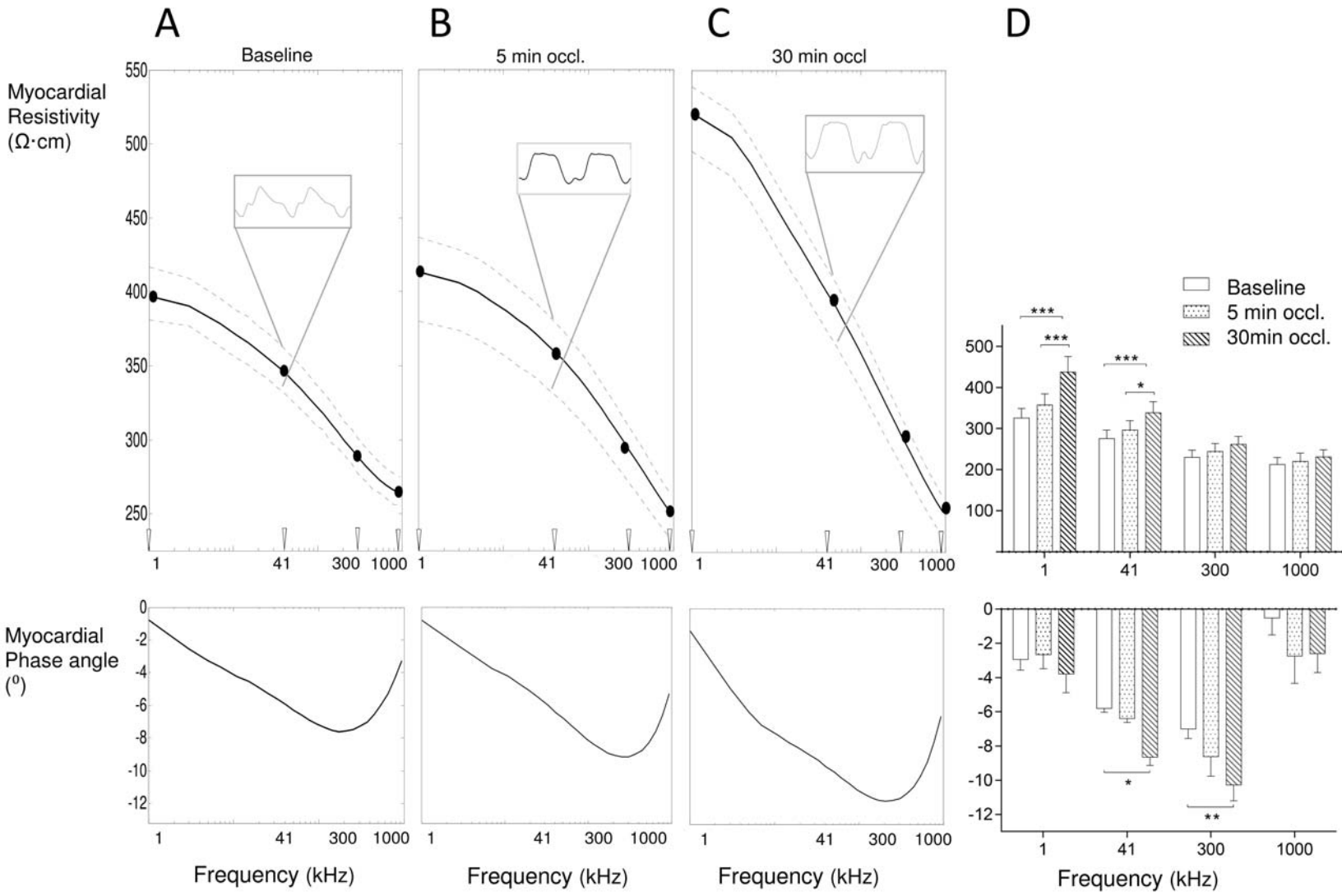
A
B
C
D
Baseline
5 min occl.
30 min occl
Myocardial Resistivity (Ω·cm)
550
500
450
400
350
300
250
1
41
300
1000
Myocardial Phase angle (°)
0
-2
-4
-6
-8
-10
-12
Frequency (kHz)
Baseline
5 min occl.
30min occl.
***
*
**

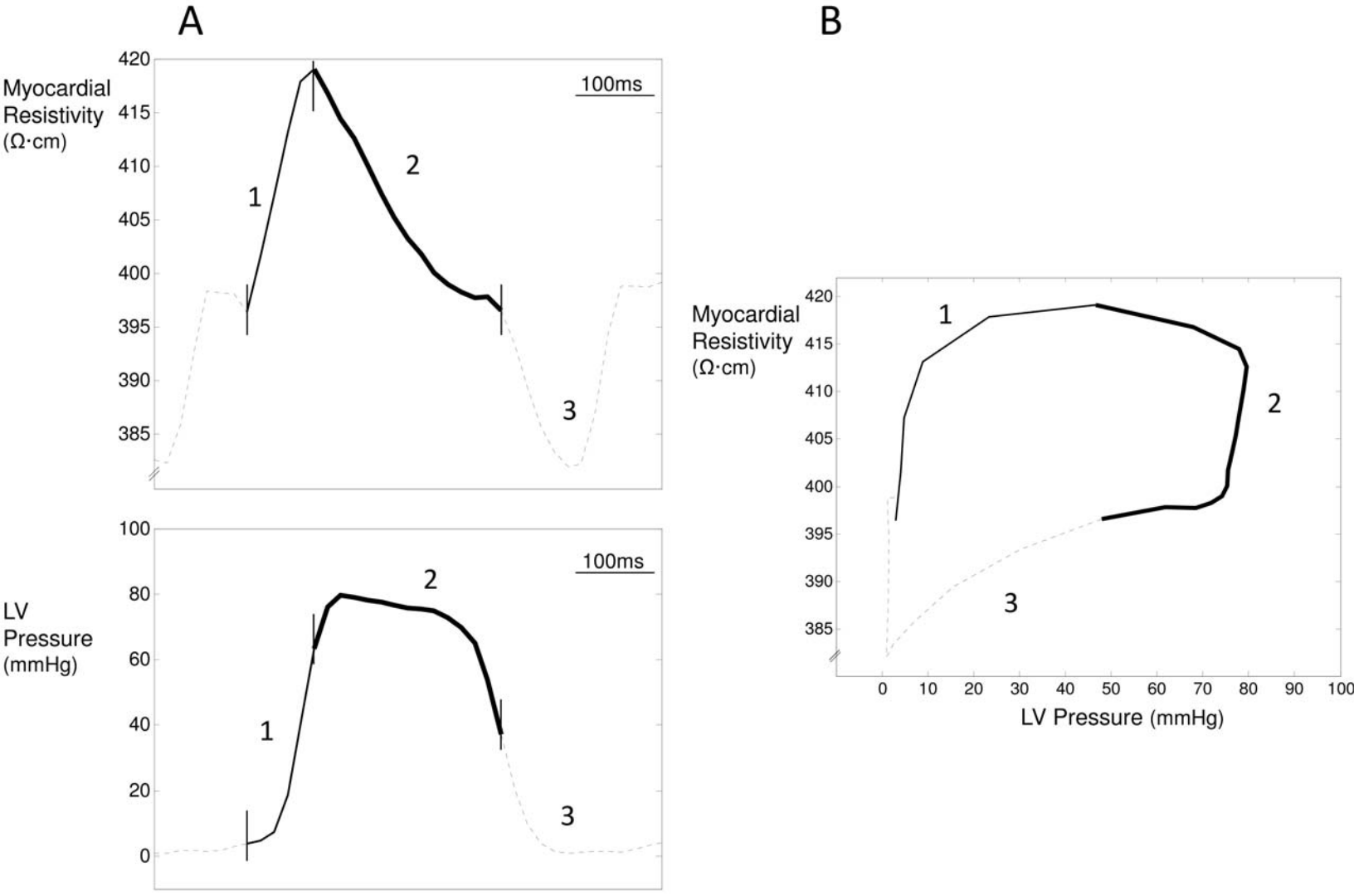
A
B
Myocardial Resistivity (Ω·cm)
420
415
410
405
400
395
390
385
100ms
1
2
3
LV Pressure (mmHg)
100
80
60
40
20
0
0
10
20
30
40
50
60
70
80
90
100
LV Pressure (mmHg)

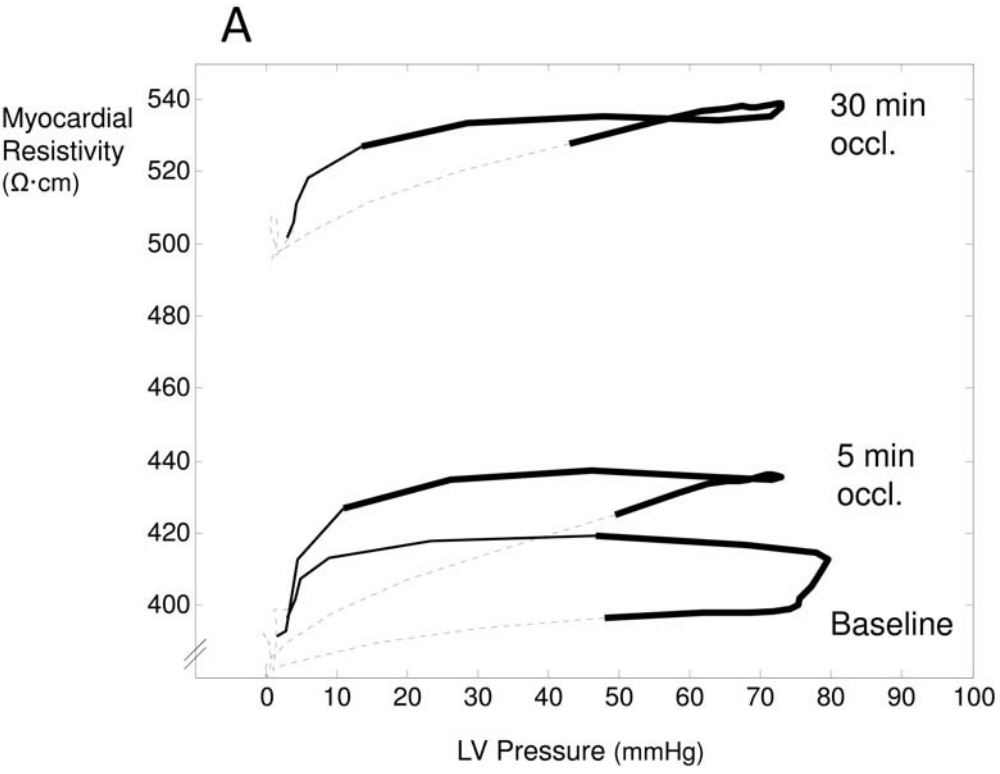
A
Myocardial Resistivity (Ω·cm)
540
520
500
480
460
440
420
400
30 min occl.
5 min occl.
Baseline
0
10
20
30
40
50
60
70
80
90
100
LV Pressure (mmHg)

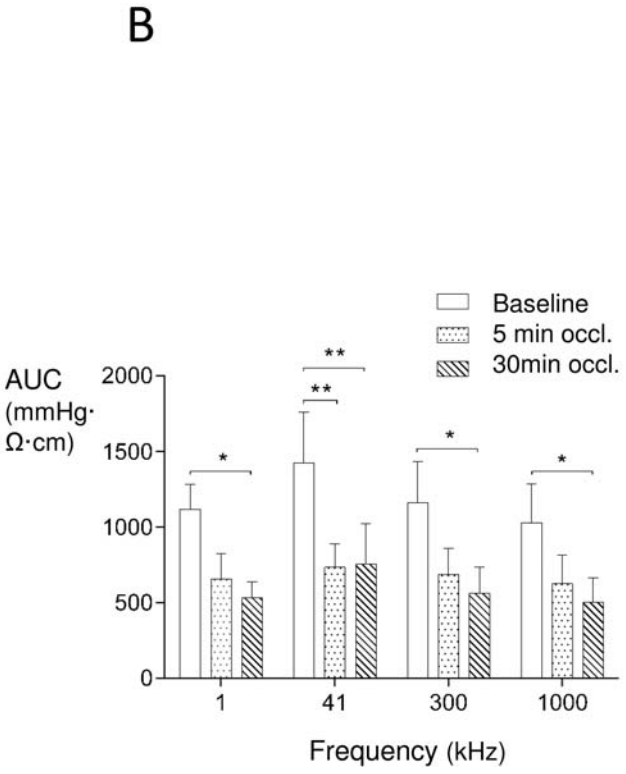
B
Baseline
5 min occl.
30min occl.
AUC (mmHg·Ω·cm)
2000
1500
1000
500
0
**
**
*
*
*
1
41
300
1000
Frequency (kHz)